JMBFS
Journal of Microbiology, Biotechnology and Food Sciences
International peer-reviewed scientific online journal

Published by Faculty of Biotechnology and Food Sciences

POWERFUL ANTIFUNGAL NANOCOMPOSITE FROM AMLA-SYNTHESIZED SELENIUM NANOPARTICLES AND NANOCHITOSAN TO PROTECT STRAWBERRY FROM GRAY MOLD

Ahmed A. Tayel[1,], Asmaa M. Otian[1], Aya M. Ebaid[2], Hoda Mahrous[2], Mohamed F. Salem[3], Madeha O. I. Ghobashy[4,5], Nurah M. Alzamel[6], Khaled E. Mazrou[7]*

Address(es): Prof. *Ahmed A. Tayel*,
[1] Department of Fish Processing and Biotechnology, Faculty of Aquatic and Fisheries Sciences, Kafrelsheikh University, Kafrelsheikh City 33516, Egypt
[2] Department of Industrial Biotechnology, Genetic Engineering and Biotechnology Research Institute, University of Sadat City, El-Sadat City 32897, Egypt
[3] Department of Environmental Biotechnology, Genetic Engineering and Biotechnology Research Institute, University of Sadat City, El-Sadat City 32897, Egypt
[4] Department of Microbiology, Faculty of Science, Ain Shams University, Cairo, Egypt
[5] Department of Biology, Biodiversity Genomics Unit, Faculty of Science, University of Tabuk, 71491, Tabuk, Saudi Arabia
[6] Department of Biology, College of Science and Humanities, Shaqra University, Shaqra 11961, Saudi Arabia
[7] Department of Plant biotechnology, Genetic Engineering and Biotechnology Research Institute (GEBRI), University of Sadat City, El-Sadat City 32897, Egypt

*Corresponding author: ahmed_tayel@fsh.kfs.edu.eg

https://doi.org/10.55251/jmbfs.11934

ARTICLE INFO

Received 11. 10. 2024
Revised 23. 1. 2025
Accepted 31. 1. 2025
Published xx.xx.201x

Regular article

OPEN ACCESS

ABSTRACT

Strawberry fruits (*Fragaria x ananassa*) are very perishable and susceptible to fungal deterioration, mainly by *Botrytis cinerea* (grey mold). The amla (*Phyllanthus emblica*) fruits' extract (AmE) was employed for biosynthesizing selenium nanoparticles (SeNPs) and their nanoconjugates with nanochitosan (NCT) were constructed, characterized and assessed as potential antifungal composites to control *B. cinerea* and suppress grey mold development in strawberry fruits. The AmE- synthesized SeNPs had mean diameter of 10.23 nm; their nanoconjugates with NCT were validated using UV analysis, electron microscopy and infrared spectroscopy (FTIR). The NCT/AmE/SeNPs nanoconjugates had mean diameters of 132.71, 135.18 and 149.37 nm for the formulations T1 (2NCT:1AmE/SeNPs), T2 (1NCT:1AmE/SeNPs) and T3 (1NCT:2AmE/SeNPs), respectively. The treatment of *B. cinerea* with fabricated nanocomposites led to severe distortion and lysis of fungal mycelium throughout treatment for 30 h; T2 formulation was the most powerful followed by T1 formulation. Coating of experimentally infected strawberry fruits with NCT/AmE/SeNPs nanoconjugates could uphold the freshness and natural appearance of fruits for more than 10 days at 27±2 °C and 90% relative humidity. The fabrication and application of NCT/AmE/SeNPs could be promisingly advised as effective edible antifungal agent to control gray mold infection of crops.

Keywords: Biosynthesis; *Botrytis cinerea*; Nanoconjugation; Nanomaterials; Postharvest

INTRODUCTION

Fruits are seriously threatened by numerous biological and environmental factors after harvesting; phytopathogens are from the most threats beside the respiration levels and physical damages **(Ali *et al*., 2022**; **Bahmani *et al*., 2022)**. Postharvest deterioration models involve physiological changes, material losses, metabolic changes, and pathological degradation. **(Finardi *et al*., 2022; Sengun *et al*., 2022).** Among the primary causes for postharvest collapses is postharvest deterioration transported by *Botrytis cinerea* (grey mold). More than 200 crops are affected by this necrotrophic, airborne fungus, with pome fruits, berries, grapes, and stone fruits being the main targets. The signs of the disease can vary greatly, but the majority of them involve soft rots that are followed by parenchyma tissues that have been saturated with water and grey masses of conidia **(Najjar and Abu-Khalaf, 2021).** These signs of fruit degradation diminish their marketability. These illnesses harm the fruits' capacity to be stored and negatively impact their ability to be sold **(Tripathi *et al*., 2004).** The fruits of strawberry (*Fragaria x ananassa* Duch.) are the predominantly consumed berries, due to elevated nutritional/phytochemicals' concentration and their distinct flavor **(Oszmiansk *et al*., 2009).** Strawberry fruits, due to physical characteristics and high respiration rate, are exceedingly exposed to higher postharvest losses. Fruits are furthermore mostly endangered by phytopathogens; *B. cinerea* fungus is frequently responsible for most of strawberry deteriorations **(Caleb *et al*.,2016).** As a result, new technologies that can aid in reaching these objectives are constantly being sought for. One of the most significant advancements that has previously been used in this field is nanotechnology **(Zorraqun-Pea *et al*., 2020, Zorraquín-Peña *et al*., 2020)**.

Chitosan; the natural biopolymer with exceptional biological and film-forming competences, can be meritoriously applied in food sectors with highest biosafety, biodegradability and biocompatibility (**Hegde and Selvaraj, 2024**). Chitin, the primary component of crustacean exoskeletons, is deacetylated to produce chitosan (CT), a polysaccharide that can be obtained **(No *et al*., 2002*)***. The exoskeleton of some insects and the mycelia of some fungus can both contain chitin and CT **(Begum *et al*., 2023)**. CT exhibits a wide range of astounding biological functions, such as metal chelation, antioxidation, and microbial pathogen (fungi, yeast, and bacteria) inhibition of cancerous cells **(Tayel *et al*., 2010)**. According to reports from sources such as **(No *et al*., 2002, Tayel *et al*., 2010*)***, CT is an effective antibacterial substance (against both Gram^{+ve} and Gram^{-ve} bacteria). Nanoparticles of chitosan (NCT) are nanoparticles that share characteristics with chitosan biopolymers, such as quantum size effects, and they have a variety of uses as antibacterial agents **(No *et al*., 2002; Hegde and Selvaraj, 2024)**. Particle size reduction and an increase in the unique physical and chemical characteristics of NCT are caused by the surface-to-particle size ratio in nanoparticles **(Roy *et al*., 2019)**. Together with the original CT bioactive features, NCT exhibit the small size, quantum size effects, surface and contact effect, and other characteristics of nanoparticles **(Begum *et al*., 2023).** There are many ways to make NCT, but the most popular one is the sodium tripolyphosphate (TPP) and CT ionotropic gelation. NCT were widely used for the efficient delivery of bioactive chemicals and as controlled-release medication carriers **(Almutairi *et al*., 2020)**.

Due to its traditional medicinal uses, amla (*Phyllanthus emblica* Linn) fruits have numerous health, cosmetic and nutritional applications (**Yokozawa *et al*., 2007**). Amla fruits contain diverse nutrients and phenolic components, e.g. vitamin C, minerals, tannins, curcuminoids, rutin, and phyllembilic acid (**Fujii *et al*., 2013**). According to several studies, amla is a strong contender against oxidative stresses (**Kim *et al*., 2005**; **Yokozawa *et al*., 2007**; **Sharma *et al*., 2009; Reddy *et al*., 2010**). It also boosts the levels of antioxidant enzymes like catalase, superoxide dismutase, Glutathione (GSH) reductase, GSH peroxidase, and GSH S-transferase and enables the antioxidant defense mechanism **(Shukla, Vashistha, & Singh, 2009)**. The market for herbal medicines has seen an increase in interest recently. The anticipated annual market value for this class of medications is US$ 20 million **(Dutra *et al*., 2016).** Hence, it is necessary to acquire standardized extracts **(Noriega *et al*., 2012).** The manufacture of standardized extracts is dependent upon accurate knowledge of the cultivation, extraction, and purification processes as well as plant species identification conditions, and monitoring of the quantity of chemical markers present. Pharmaceutical goods with a superior caliber, specific

safety and therapeutic efficacy requirements, and standardized plant extracts are produced as a result **(Kunle *et al*., 2012; Bezerra *et al*., 2017).**
Selenium, the vital element for higher organisms, should be provided to humans in daily doses of 40- 300 µg. Se at these quantities is required for the typical upkeep of organisms' functions, but at large dosages (3,200 µg/day), it may be harmful **(Zhao *et al*., 2018).** The Se nanostructures, which include trigonal nanoplates, hexagonal prisms, spheres, nanorods, and nanowires, potentially, nevertheless, reduce the Se danger and toxicity, allowing for effective employment in biomedical/pharmaceutical agents **(Kumar and Prasad 2020)**. The greenly synthesised SeNPs, particularly those using extracts from plants, were actually used in pharmaceutical formulations for antioxidant and anticancer as well as edible coating (EC) preservatives for agricultural crops and animal items **(Dobrucka *et al*., 2014; Sonawane *et al*., 2018**; **Menon *et al*., 2020,)**.
Accordingly, we targeted the employment of Amla extract (AmE) for biosynthesizing SeNPs and their nanoconjugates with NCT are constructed, characterized and valuated as antifungal composites to control *B. cinerea* and suppress grey mold development in strawberry fruits.

MATERIAL AND METHODS

Preparation of Amla (AmE) extracts

In the Arab Republic of Egypt, dried (Amla) was purchased at a neighborhood shop (ARE). The plant materials were ground to a size of 60 mesh, soaked in eight folds (w/v) of 70% ethanol, Sigma-Aldrich, MO, and agitated at 160 x speed for 22 hours at room temperature (RT; 25 ± 2 °C). The plant remnants were eliminated using filtration, after which the AmE extract was dried by rotary evaporation (IKA, RV 10, Germany). A concentration of AmE (1 mg/mL) was prepared in aqueous Tween 80 solution (2%, v/v) and used for further trials **(Tayel *et al*., 2020)**.

The production of selenium nanoparticles (SeNPs) in Amla

Fresh sodium selenite "Na_2SeO_3, Sigma-Aldrich, MO" aqueous solution (10 mM) was made in DW. Then, 10 mL of the AmE (1%, w/v) and Na_2SeO_3 solution (10 mM) were mixed together while being stirred at 610 xg for 55 minutes at RT using an AREX-6 magnetic stirrer from VELP Scientifca Srl, Italy. The eyesight perception of a solution with a brownish-orange color indicated the AmE production of SeNPs. The mixture is then vacuum-dried at 43 °C in rotary evaporator. The AmE/SeNPs solution is then prepared via dissolving and sonication in deionized water (DW).

Synthesis of Chitosan/AmE/SeNPs

The production of NCT and its loading with AmE required the creation of the following solutions, according to **Almutairi *et al*. (2020**): AmE (1 mg/mL in 2% Tween 80 solution in DW), TPP, Sigma-Aldrich, MO (0.5 mg/mL in DW), and CT (1 mg/mL in 1% acetic acid solution). After the pH of the CT solution was adjusted to 5.2, the TPP solution was progressively added to the CT solution using a syringe needle at a rate of 0.35 mL/min until the volume of both solutions was equal. Prior to TPP dropping, the aforementioned procedures were used to create CT/AmE-SeNPs while incorporating an equivalent volume of AmE/SeNPs into NCT, before TPP dropping.

Characterization of synthesized nanoparticles

UV-visible (UV-vis) analysis

Using a UV-visible spectrophotometer, the (AmE/SeNPs) solution's spectrum was captured (model UV-2450, Shimadzu, Japan). The absorbance was measured between 200 and 500 nm. The absorbance peak could be seen.

Transmission electron microscopy (TEM) imaging

With the use of a TEM (JEOL Ltd., JEM-2100, Japan) running at 200 kV of acceleration voltage, the morphological and size of the phytosynthesized (AmE/SeNPs) were evaluated. The reaction solution was sonicated for 10 minutes (Branson-sonifier 250, USA) after being diluted with DW. After the sample had been sonicated, it was drop-coated onto copper grids that had been coated with carbon, After 30 minutes of vacuum drying, electron micrographs were produced. Furthermore, the structure and morphology of NCT/AmE/SeNPs nanocomposite were screened via scanning (SEM) electron microscopy (JEOL, IT100, Japan) after dehydrating samples and coating with gold/palladium.

Particles' size and Zeta potential (ζ)

After the nanomaterials were dissolved and sonicated, the distribution, size, and charges of the phytosynthesized nanocomposites (AmE/SeNPs and NCT/AmE/SeNPs) were determined using photon correlation spectroscopy with Zetasizer (Malvern™, UK).

FTIR analysis

Briefly, the infrared spectra of employed materials (AmE, CT, SeNPs) and their nanocomposites were appraised via FTIR "Fourier transform infrared spectroscopy, JASCO -360, Tokyo, Japan", after mixing dried materials with potassium bromide (KBr). The transmission of compounds were plotted within wave numbers of 450–4000 cm^{-1}.

Determination of the antifungal activity

Fungal strain

The challenged phytopathogenic mold were *Botrytis cinerea* strains (*B. cinerea* A and *B. cinerea* I), e.g. ATCC-26943 and an isolate delivered from the "Egyptian Phytomicrobial Collection for Research & Sustainability Excellence Center, Kafrelsheikh University, Egypt", respectively,. After the fungi was grown for seven days at 25 °C in potato dextrose agar (PDA) medium, its features were determined using both macro and microscopic traits.

Analyzing antifungal activity in vitro

The antifungal efficacy of *B. cinerea* against NCT, AmE, AmE/SeNPs, and NCT/AmE/SeNPs was tested *in vitro*. The standard fungicide, Imazilil (Sigma-Aldrich, Taufkirchen, Germany), was diluted with 20% (v/v) dimethyl-sulfoxide (DMSO) also from Sigma-Aldrich, Germany.
The well difusion (WD) technique
The Agar WD technique is widely used to assess the antifungal potentiality, especially from natural substances. Initially, the PDA plates were inoculated and distributed using 100 µL of fungal spores' suspension. Subsequently, 6 mm diameter wells were made using cork-borers, and 50 µL of each chemical (at 1% concentrations in DW or imazilil in DMSO) was pipetted into each well. The inhibition zones (IZ) that formed around the wells on the plates were measured in millimeters after they were incubated at 27 °C for 72 hours in the dark (**Gan *et al*., 2020; Tayel *et al*., 2024**).

Minimum fungicidal concentration (MFC)

To ascertain the antifungal efficacy of AmE/SeNPs, NCT, and their composites against *B. cinerea*, the agar macro-dilution method was utilized. Melted PDA was used to create serial dilutions, which were then placed into sterilized Petri dishes. Once the dilutions had hardened, 100 µL of the *B. cinerea* spore suspension (equivalent to ~2 X 10^5 spore/mL) were spread out onto the plates, and the plates were incubated for seven days at 25±1 °C. The lowest concentration in PDA that totally prevents fungal growth upon incubation is known as the least inhibitory concentrations, or MIC, for the compounds under study. Using the diluted broth method, **(Jorgensen *et al*., 2009; Tayel *et al*., 2016)** In relation to *B. cinerea* isolates, the MFC of each screening chemical (NCT, AmE, AmE/SeNPs, and NCT/AmE/SeNPs) or imazilil was assessed. Gradual amounts (10–100 mg/mL) of screened substances were mixed with PDB "potato dextrose broth medium" and imbibed with *B. cinerea* spores. Following an 8-day aerobic incubation of the media, new PDA plates were filled with 100 µL of each trial and left to incubate. After incubating for seven days, the MFC from each chemical toward the fungal isolates was determined by looking for any established cells on PDA plates. The MFC ranges used to discriminate between *B. cinerea* isolates that were susceptible and those that were resistant were as follows: very susceptible at 25 mg/mL, moderately susceptible at 25–50 mg/mL, partially resistant at 50–75 mg/mL, and resistant at >75 mg/mL.
Microscopic remarks of treated fungal mycelia with nanocomposite
The alterations/deformation of *B. cinerea* mycelial morphology, after their exposure to NCT/AmE/SeNPs (at relevant MFC in PDB), were microscopically visualized "Labomed Lx400; Labo America, Fremont, CA". The mycelia were incubated in nanocomposite-amended broth for 10, 20 and 30 h under gentle stirring. The exposed mycelia were mounted and tarnished using lactophenol-blue, then inspected and photographed.

Preparation of Edible Coating (EC) Solution

For EC solutions' preparation, the invented compounds/nanocomposites (NCT, AmE/SeNPs and NCT/AmE/SeNPs) were dispersed in sterilized DW at RT, with 1.0 % concentration (w/v) and ultrasonicated pending full dissolution. The plasticizer (e.g. glycerol) was adjoined at 0.25% ratio (v/v) to the EC solutions and stirred until homogenous solution was attained **(Tayel *et al*. 2016; Youssef *et al*., 2022)**.

Coating and inoculation of strawberries

At Kafrelsheikh University in Egypt, the KFS research farm cultivated and gathered fresh strawberries (*Fragaria* × *ananassa*). Fruits that were free of obvious rot or flaws and had uniform size, color, and maturity (~75 percent full red color) were chosen. After carefully washing with DW, the strawberries were immersed

in a 250 ppm sodium hypochlorite solution for 20 seconds and then rinsed with DW. To ensure that there was no residual chlorine, a chlorine test kit (Pocket Colorimeter™, Hach Co., Loveland, Colo., U.S.A.) was utilized. Infection was made by immersing the strawberries in the *B. cinerea* spore solution (10^4 spore/mL) for 30 seconds and drying them in a biosafety room for an hour, prior to coating application. The infected strawberries groups were dipped in coating solutions containing the MIC from NCT, AmE/SeNPs or NCT/AmE/SeNPs nanocomposite, while the control group was dipped in 1% acetic acid solution. Following a 2-hour drying period, the fruits were arranged in polystyrene (Styrofoam) plates and covered with a polyethylene layer that included venting holes (Creative Forming, Inc., Ripon, WI, USA). Strawberries were divided at random groups; after being immersed in the nanocomposite-based suspensions for two minutes and dried at 20 °C, the strawberries from each treatment groups were placed in a 200 g polypropylene container and stored at 27±2 °C and 90% relative humidity. During the seven-day storage period, fungal deterioration was visually inspected every day. Any fruit exhibiting mycelial maturity on the surface was deemed to have decayed.
The average fungal lesions (LD, %) diameters were regularly assessed throughout incubation (**Salem *et al*., 2022a; 2022b**). Each treatment group included 15 fruits and their mean LDs within groups were gauged.

Analytical statistics

Utilizing the SPSS package (SPSS V-11.5, Chicago, IL, USA), the mean values ± standard deviation (SD) of triplicated trials were calculated. The significances of the results at $p < 0.05$ were calculated with one-way ANOVA and the t-test.

RESULTS AND DISCUSSION

Biosynthesis of SeNPs

AmE bioreduced Na_2SeO_3 to SeNPs, and after 30 minutes, the solution's color gradually changed from pale yellow to deep brownish orange, indicating the biosynthesis of SeNPs (**Kumar and Prasad 2020; Menon *et al*., 2020**). **Figure 1** shows this progression. Recent research on the synthesis and capping of SeNPs using various polysaccharides and biopolymers (**Shi *et al*., 2020; ElSaied *et al*., 2021**) indicates that the peak of the UV-vis curve for NPs, known as λmax, was determined at 262 nm (2 in **Figure 1**). More color depth in NPs solutions indicated smaller sizes of synthesized NPs, and color revolutions of NPs synthesizing solutions are primarily linked to the stimulation of surface plasmon resonance in synthesized NPs **(Tsekhmistrenko *et al*., 2021).** The presented SeNPs phytosynthesis procedure is economical, straightforward, and environmentally benign; the produced NPs are thought to be safe, nontoxic, and extremely stable **(Zonaro *et al*., 2015).** SeNPs' color variations during synthesis and their relationship to Ps were described **(Tsekhmistrenko *et al*., 2021).**

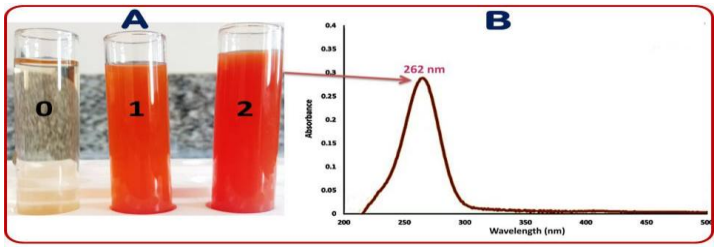

Figure 1 Color indicators of Amla extract-mediated SeNPs synthesis: (A) final appearance following 0 (0), 15 (1), and 30 min (2) of incubation; and (B) UV-Vis spectrum of the biosynthesized SeNPs.

FTIR Analysis

Through their FTIR spectra, the produced compounds' biological groups, linkages, and interactions are identified **(Figure 2)**. Typical bands could be seen at wavenumbers 3453.7 cm^{-1} (O–H stretch), 2887.4 cm^{-1} (C–H stretch), 1623.2 cm^{-1} (N–H bend), 1375.3 cm-1 (bridge O stretch), and 1137.8 cm^{-1} (C–O–C bonds) in the pure NCT spectrum (**Figure 2**, NCT), which mirrored the FTIR spectra of pure powder. The C–O stretch of glycosidic bonds was attributed to the bands at wavenumber 1052.5 cm^{-1} **(Tayel *et al*., 2014; Alkhatib *et al*., 2023)**. The CT absorption band resembled the CT absorption band. After the deacetylation process, there were variations in the absorption spectra at 1688.7 cm^{-1} from the C–O stretch **(Potrc *et al*., 2020)**, which caused the variances. Between 1650 and 600 cm^{-1} was where the distinctive AmE fingerprints were most prevalent **(Figure 2, AmE)**. Aldehyde carbonyl C–O 's stretching vibration gave rise to the peak at 1604.3 cm^{-1}. Alcohol C–OH showed a usual peak at 1447.7 cm^{-1}.

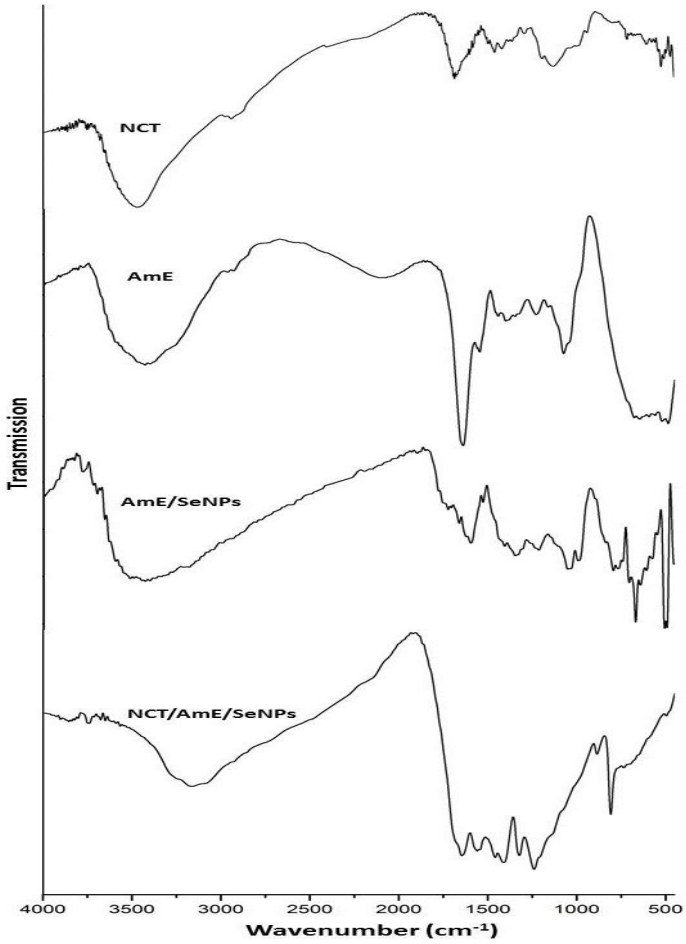

Figure 2 The produced selenium nanoparticles with Amla extract (AmE/SeNPs), their nanocomposites with nano-chitosan (AmE/Se/NCT), and the plain chitosan nanoparticles (NCT) and Amla extract (AmE) FTIR spectra.

The stretching vibrations of C–O and C–OH deformation were thought to be responsible for the AmE peaks at 987.4 and 1071.3 cm^{-1}. For in-plane bending absorption, C–H2 alkanes that face the swing and the aromatic ring C–H were said to be responsible for the peak at 1281.9 cm^{-1} **(Potrc *et al*., 2020, Li *et al*., 2013)**. The potential biomolecules for Se+ ion reduction and capping of bioreduced SeNPs produced by photosynthesizing AmE with SeNPs have been discovered **(Bityutskyy *et al*., 2021)**. The stability of the metal NPs found in AmE and the capping agent were both determined using FTIR spectra. The detected peak designated the carbonyl group at 1651.7 cm^{-1} as well as the O–H stretching group of phenols and alcohols at 3380.4 cm^{-1} (**Gupta and Saxena, 2023**). O–H stretching caused the broad absorption band at 3410 cm^{-1} to develop. The C–O bond in AmE aldehyde was involved in the production of SeNPs as shown by the band's shift from 1651.3 cm^{-1} (in AmE) to 1718.7 cm^{-1} (in AmE/SeNPs spectrum). The nitro compounds were represented by the band at 1350.2 cm^{-1}. Due to the influence of the aromatic ring and conjugation, this band was wider than it would normally be for aldehyde compounds. The aromatic C–C bending caused the band at 1350 cm^{-1}, while the C–O stretching caused the band at 1050 cm^{-1} **(Goyal etal.,2019)**. The primary distinguishing peaks from each individual agent were present in the FTIR spectrum of the AmE/Se/CT nanocomposite, suggesting the physiochemical interactions between these components as seen by the shifts and changes in the transmission intensities of the distinctive bands.

Particles size and Zeta potential

Table 1 evaluates the Ps dispersion and their zeta potential for the synthesized NCT, AmE/SeNPs, and AmE /SeNPs/NCT. AmE's ability to produce SeNPs with a mean diameter and minute Ps range was demonstrated. The NCT (with mean Ps of 132.71nm) had high positive surface charges (+23.61 mV), while the phytosynthesized SeNPs had negative Z-potential (+32.25 mV). The significantly greater Ps range and mean diameters of the nanocomposites of both NP types (AmE /SeNPs/NCT) indicate their mating and mixing. The investigated NPs' great stability in solutions was demonstrated by the Z-potential that was obtained. These results corroborated earlier studies (**Chen *et al*., 2018**) that revealed the synthesis of CT and SeNPs nanocomposites with high constancies and minute Ps.

Table 1 The zeta potential and size distribution for Amla /SeNPs/NCT nanoformulations (T1, T2 and T3), Amla/SeNPs (TS), and plain NCT (T0)

Code	Chitosan: Amla/SeNPs ratio	Particles size range	Particles size mean	Zeta potential (mV)
TS	0:1	1.21-29.53	10.23	-26.21
T0	1:0	70.63-192.84	126.65	+ 32.25
T1	2:1	68.45-208.69	132.71	+ 23.61
T2	1:1	77.83-213.22	135.18	- 13.09
T3	1:2	81.68-224.75	149.37	- 26.42

Electron microscopy analysis of nanomaterials

The TEM images of AmE/SeNPs produced during phytosynthesis demonstrated the uniform distribution of NPs and their stability with AmE during phytosynthesis. SeNPs had practically no aggregation and were spherical in form **(Figure 3-A)**. According to earlier research utilizing different plant extracts **(Al-Saggaf *et al*., 2020),** tiny AmE particles were seen in the AmE/SeNPs matrix together with SeNPs. Depending on the phytochemical reduction agents employed, previous studies looked at using plant derivatives to produce different SeNPs particle sizes and morphologies. According to **Tayel *et al*. (2024**), the extraction of fenugreek seeds produced SeNPs with a smooth oval form and Ps of 50-150 nm, while **Sharma *et al*. (2014**) found that the dried raisin extract produced Se nanoballs measuring 3-18 nm. *Bougainvillea spectabilis* flowers have spherical-shaped SeNPs with Ps ranging from 18 to 35 nm (**Menon *et al*., 2019**), and microbial phytosynthesis produced spherical NPs with larger Ps (**Al-Saggaf *et al*., 2020; Menon *et al*., 2019**). The biomolecules and a number of organic chemicals present in plant extracts, such as AmE, may reduce and stabilize NP levels and prevent their aggregation **(Menon *et al*., 2019)**.

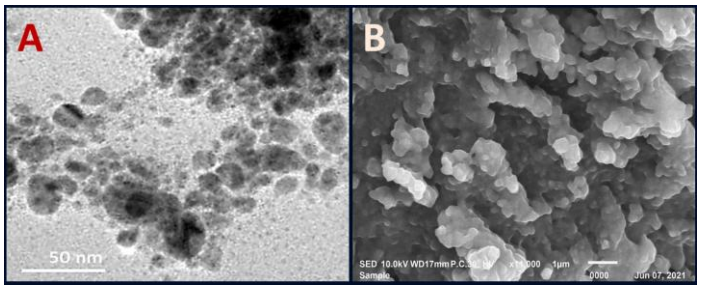

Figure 3 Electron microscopy imaging of nanomaterials including TEM micrograph of phytosynthesized SeNPs with AmE (A) and SEM imaging of nanocomposite from nanochitosan and AmE/SeNPs (B).

Using the SEM method, the size and structure of the NCT/AmE/SeNPs were observed (**Figure 3-B**). NCT/AmE/SeNPs formation and their morphological dimension, with an average diameter of 132.12 nm were observed, which is in accordance with former findings regarding the NCT-based nanocomposites **(Alotaibi *et al*., 2019; Alsaggaf *et al*., 2020; Tayel *et al*., 2020; Salem *et al*., 2022; Youssef *et al*., 2022)**.

Antifungal potentiality of nanomaterials

The anti-*B. cinerea* potentialities of screened compounds (AmE, NCT, AmE/SeNPs and NCT/AmE/SeNPs), compared to imazilil, were emphasized in **Table 2**. The nanocomposites (NCT/AmE/SeNPs) were significantly the most forceful toward both *B. cinerea* strains, concerning their IZs and MFCs values. T2 formulation was the most effective antifungal nanocomposite followed by T1 formulation then T3 formulation (**Table 2**). Additionally, the T2 and T1 nanocomposites exhibited comparable and stronger antifungal actions than imazilil (standard fungicide), as these NCT/AmE/SeNPs formulations have wider IZs and lower MFCs than imazilil. The next powerful agent after NCT/AmE/SeNPs formulations was the AmE/SeNPs complex, followed by NCT then plain AmE (**Table 2**). The *B. cinerea* A strain was predominantly more sensitive than *B. cinerea* I strain, toward most screened agents. The antifungal synergism between NCT, AmE and SeNPs was evidenced, as the nanocomposite had more biocidal action than each individual component, which was stated for other NCT-based antifungal nanocomposites (**Alotaibi *et al*., 2019**; **Alsaggaf *et al*., 2020**, **Salem *et al*., 2022a**; **Salem *et al*., 2022b; Abd-Elraoof *et al*., 2023; Tayel *et al*., 2024**). The utilizations of NCT to carry, cap and deliver extra active biomolecules such as plant derivatives and biosynthesized nanometals were reported to boost their collective actions as antioxidative, anticancerous and antimicrobial nanocomposites [**Salem *et al*., 2022b; Abd-Elraoof *et al*., 2023**]. The earlier findings verified the potential NCT role for strengthening the fungicidal actions of AmE and SeNPs. The NCT charged (positively) particles capable of attaching fungal hyphae and interacting with mycelial membranes; their penetration through such membranes triggers the inhibition/destruction of microbe's biosystems and their cellular lysis (**Alsaggaf *et al*., 2020**, **Salem *et al*., 2022a**; **Tayel *et al*., 2024**).

Table 2 Antifungal activities of amla extract (AmE), AmE-mediated SeNPs, and their composites with nanochitosan (NCT/AmE /SeNPs) against *Botrytis cinerea* strains

Antifungal substance	***B. cinerea* A**		***B. cinerea* I**	
	IZ (mm)*	**MFC** (mg/L)	**IZ** (mm)	**MFC** (mg/L)
NCT	14.8±1.8^{a}	45.0	13.9±2.1^{a}	45.0
AmE	13.1±2.1^{a}	47.5	12.4±2.2^{a}	50.0
AmE/SeNPs	19.3±2.8^{b}	35.0	19.6±2.6^{b}	35.0
NCT/AmE/SeNPs (T1)	23.4±3.5^{c}	30.0	21.8±3.3^{c}	32.5
NCT/AmE/SeNPs (T2)	25.6±3.3^{c}	27.5	23.3±3.6^{c}	30.0
NCT/AmE/SeNPs (T3)	21.1±3.0^{c}	32.5	20.2±2.8^{c}	35.0
Imazilil	22.6±2.4^{c}	30.0	20.5±2.3^{b,c}	32.5

* Values are triplicates' means ± deviation; dissimilar superscripted letters in distinct column assign significance at $p > 0.05$.

Examination of treated fungal mycelia under a microscope

Following treatment with MFC from T2 formulation of NCT/AmE/SeNPs, a change in the morphology of the *B. cinerea* mycelial was observed under a microscope (**Fig. 4**).

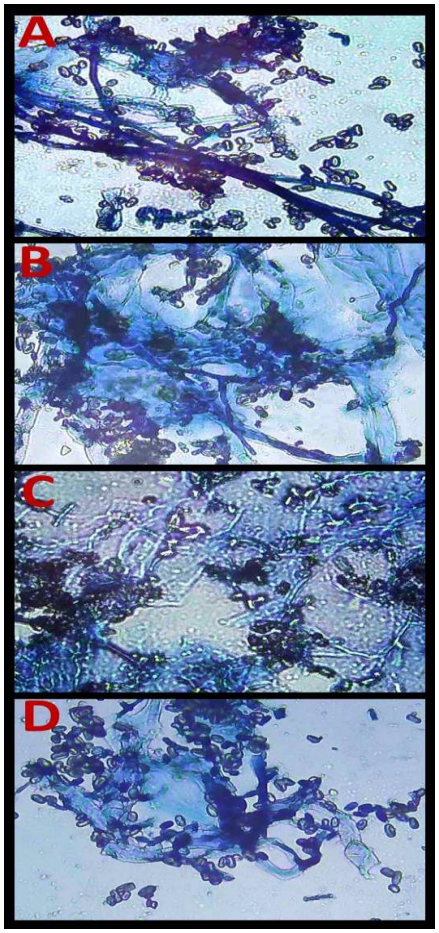

Figure 6 *Botrytis cinerea* mycelial growth in supplemented broth with nanocomposite from chitosan and SeNPs synthesized with amla extract for 10 h (B), 20 h (C) and 30h (D), compared with normal hyphal growth (A).

At the onset of the experiment, the fungal mycelium exhibited robust and healthy characteristics. Its wall and surface were smooth and dense, devoid of any visible deformities (**Fig. 4-A**). The mycelium exhibited erratic swellings and fragmentations, softening of their walls, and the emergence of distortion indications after ten hours of exposure (**Fig. 4-B**). The fungal mycelia were largely lysed and had lost their characteristic features with the extension of exposure time, up to 20 hours. At this point, the internal cell components were seeping out of the hyphae (**Fig. 4-C**). After 30 h of exposure (**Fig. 4-D**), the fungal mycelia were entirely lysed, fractured and fragmented into tiny parts due to nanocomposite actions.

The inventive NCT/AmE/SeNPs nanocomposite presented here is proposed to act through manifold mechanisms; 1: NCT particles could carry/encapsulate AmE/SeNPs toward the fungal mycelia then 2: nanocomposite can attach/interact with their membranes to trigger their tempering and fractional lysis, then 3: after nanocomposite penetration through the hypha, the AmE/SeNPs are liberated from NCT to interact with organelles/biosystems inside hypha and overwhelm their functions (**Alotaibi *et al*., 2019**; **Salem *et al*., 2022a**; **Salem *et al*., 2022b; Abd-Elraoof *et al*., 2023; Tayel *et al*., 2024**). These mechanisms can consequently trigger fungal deformation, destruction and lysis. The proposed antifungal mechanisms of SeNPs included the generation of ROS "reactive oxygen species" that perform vital roles in cellular apoptosis, biotoxicity, accumulative leakage of cytoplasmic content, promotion of DNA oxidative damage, and cell wall destruction (**Salem *et al*., 2022a**; **Hamouda *et al*., 2024**).

Application of an edible coating based on NCT to strawberries

The effects of strawberry fruits treated with NCT-based edible coatings (e.g., plain NCT, NCT/AmE, and NCT/AmE/SeNPs) are photographed after 10 days of infection with *B. cinerea* (**Figure 5**). The coated fruits showed less infection indications than the uncoated control fruits, which eventually entirely decomposed and were covered with fungal growth **(Figure 5-C)**. The strawberry fruits were entirely shielded from any infestation indications and retained their fresh-looking texture after being coated with an NCT/AmE/SeNPs-based solution (**Fig 5-T3**). Compared to NCT/AmE-coated fruits, where the fungal infestation only covered 9.2±1.5% of the fruit's surface area (**Fig 5-T2**), and the infection signals on NCT-coated fruits covered 52.3±6.5% of it **(Figure 5-T1)**. It's interesting to note that the NCT/AmE/SeNPs nanocomposite coating on the fruits was able to keep the quality of the coated fruits without showing any signs of infection for an additional 20 days after the experiment's completion.

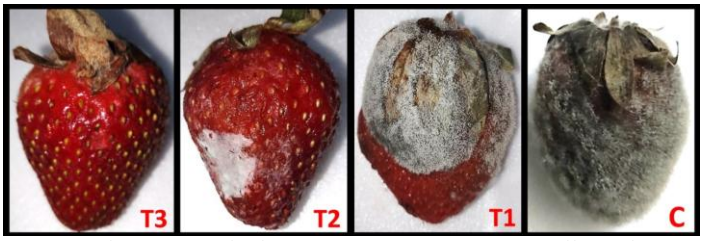

Figure 5 After 10 days of infection with *Botrytis cinerea*, the effects of coating strawberry fruits with formulated nanochitosan (T1), Amla extract/SeNPs (T2), and nanochitosan/Amla extract/SeNPs (T3) compared to untreated fruit (C).

The chitosan and NCT-based coatings, especially those incorporated with additional nanoparticles, provided excellent barriers around coated fruits, which hinder the gases passage (CO_2, O_2, and water vapor) (**Vlčko *et al*., 2022**; **Hamouda *et al*., 2024**). In addition to potent antifungal actions, the nanoparticle (e.g. NCT and SeNPs) coatings can also prevent the oxidative stresses on fruits (e.g. oxidation of strawberry anthocyanins) and protect fruits decomposition via guarding surface tissues and providing gas barriers (**Ali *et al*., 2022**; **Bahmani *et al*., 2022; Hamouda *et al*., 2024**).

CONCLUSION

Targeting the protection of strawberry from gray mold decay, AmE was employed for biosynthesis of SeNPs, and their conjugation with NCT was applied as edible coating for fruits. The biosynthesis, characterization and bioactivities of nanomaterials were verified, with potent antifungal actions against *B. cinerea* and minute sizes of their particles. The coating of strawberry with NCT/AmE/SeNPs nanocomposite could be recommended as bioactive edible approach for complete protection of fruits from gray mold and extension of their storage with high quality.

Acknowledgments: "The authors declare their appreciation and foremost gratefulness to ALLAH for the merciful and generous guiding throughout this work"**.**

REFERENCES

Abd-Elraoof, W. A., Tayel, A. A., Shaymaa, W., Abukhatwah, O. M. W., Diab, A. M., Abonama, O. M., ... & Abdella, A. (2023). Characterization and antimicrobial activity of a chitosan-selenium nanocomposite biosynthesized using Posidonia oceanica. *RSC advances*, *13*(37), 26001-26014. DOI: 10.1039/D3RA04288J

Ahmad, M. S., Yasser, M. M., Sholkamy, E. N., Ali, A. M., & Mehanni, M. M. (2015). Anticancer activity of biostabilized selenium nanorods synthesized by Streptomyces bikiniensis strain Ess_amA-1. *International journal of nanomedicine*, 3389-3401. doi: 10.2147/iJN.S82707

Ali, L. M., Ahmed, A. E. R. A. E. R., Hasan, H. E. S., Suliman, A. E. R. E., & Saleh, S. S. (2022). Quality characteristics of strawberry fruit following a combined treatment of laser sterilization and guava leaf-based chitosan nanoparticle coating. *Chemical and Biological Technologies in Agriculture*, *9*(1), 80. https://doi.org/10.1186/s40538-022-00343-x

Alkhatib, M., ALHusini, F., Al-Amri, M., ALHatmi, A., ALRiyami, K., & ALGhafri, M. (2023). ANTIMICROBIAL ACTIVITY OF CHITOSAN-VITAMIN E-NANOEMULSION. *Journal of microbiology, biotechnology and food sciences*, *13*(3), e10123-e10123. https://doi.org/10.55251/jmbfs.10123

Almutairi, F. M., El Rabey, H. A., Tayel, A. A., Alalawy, A. I., Al-Duais, M. A., Sakran, M. I., & Zidan, N. S. (2020). Augmented anticancer activity of curcumin loaded fungal chitosan nanoparticles. *International journal of biological macromolecules*, *155*, 861-867. https://doi.org/10.1016/j.ijbiomac.2019.11.207

Alotaibi, M. A., Tayel, A. A., Zidan, N. S., & El Rabey, H. A. (2019). Bioactive coatings from nano-biopolymers/plant extract composites for complete protection from mycotoxigenic fungi in dates. *Journal of the Science of Food and Agriculture*, *99*(9), 4338-4343. https://doi.org/10.1002/jsfa.9667

Alsaggaf MS, Tayel AA, Alghuthaymi MA, Moussa SH. Synergistic antimicrobial action of phyco-synthesized silver nanoparticles and nano-fungal chitosan composites against drug resistant bacterial pathogens. Biotechnology & Biotechnological Equipment. 2020 Jan 1;34(1):631-9. https://doi.org/10.1155/2020/8878452

Al-Saggaf, M. S., Tayel, A. A., Ghobashy, M. O., Alotaibi, M. A., Alghuthaymi, M. A., & Moussa, S. H. (2020). Phytosynthesis of selenium nanoparticles using the costus extract for bactericidal application against foodborne pathogens. *Green Processing and Synthesis*, *9*(1), 477-487. https://doi.org/10.1515/gps-2020-0038

Bahmani, R., Razavi, F., Mortazavi, S. N., Gohari, G., & Juárez-Maldonado, A. (2022). Evaluation of proline-coated chitosan nanoparticles on decay control and quality preservation of strawberry fruit (cv. Camarosa) during cold storage. *Horticulturae*, *8*(7), 648. https://doi.org/10.3390/horticulturae8070648

Begum, E. R. A., Shenbagarathai, R., Lavanya, U., & Bhavan, K. (2023). Synthesis, characterization, and antimicrobial activity of extracted chitosan-based silver nanoparticles. *Journal of microbiology, biotechnology and food sciences*, *12*(5), e4215-e4215. https://doi.org/10.55251/jmbfs.4215

Bezerra, A. N. S., Massing, L. T., de Oliveira, R. B., & Mourão, R. H. V. (2017). Standardization and anti-inflammatory activity of aqueous extract of Psittacanthus plagiophyllus Eichl.(Loranthaceae). *Journal of ethnopharmacology*, *202*, 234-240. https://doi.org/10.1016/j.jep.2017.03.029

Bityutskyy, V., Tsekhmistrenko, O., Merzlo, S., Tymoshok, N., Melnichenko, A., Polishcuk, S., ... & Yakymenko, I. (2021). BIONANOTECHNOLOGIES: SYNTHESIS OF METALSâ€™ NANOPARTICLES WITH USING PLANTS AND THEIR APPLICATIONS IN THE FOOD INDUSTRY: A REVIEW. Journal of microbiology, biotechnology and food sciences, 10(6), e1513-e1513.https://doi.org/10.15414/jmbfs.1513

Caleb, O. J., Wegner, G., Rolleczek, C., Herppich, W. B., Geyer, M., & Mahajan, P. V. (2016). Hot water dipping: Impact on postharvest quality, individual sugars, and bioactive compounds during storage of 'Sonata'strawberry. *Scientia Horticulturae*, *210*, 150-157. https://doi.org/10.1016/j.scienta.2016.07.021

Chen, W., Yue, L., Jiang, Q., Liu, X., & Xia, W. (2018). Synthesis of varisized chitosan-selenium nanocomposites through heating treatment and evaluation of their antioxidant properties. *International journal of biological macromolecules*, *114*, 751-758. https://doi.org/10.1016/j.ijbiomac.2018.03.108

Dobrucka, R. (2014). Application of nanotechnology in food packaging. *Journal of microbiology, biotechnology and food sciences*, *3*(5), 353-359.

Dutra, R. C., Campos, M. M., Santos, A. R., & Calixto, J. B. (2016). Medicinal plants in Brazil: Pharmacological studies, drug discovery, challenges and perspectives. *Pharmacological research*, *112*, 4-29. https://doi.org/10.1016/j.phrs.2016.01.021

ElSaied, B. E., Diab, A. M., Tayel, A. A., Alghuthaymi, M. A., & Moussa, S. H. (2021). Potent antibacterial action of phycosynthesized selenium nanoparticles using Spirulina platensis extract. *Green Processing and Synthesis*, *10*(1), 49-60. doi: 10.1515/gps-2021-0005.

Finardi, S., Hoffmann, T. G., Angioletti, B. L., Mueller, E., Lazzaris, R. S., HlebovÃ, M., ... & de Souza, C. K. (2022). Development and application of antioxidant coating on Fragaria spp. stored under isothermal conditions. *Journal of microbiology, biotechnology and food sciences*, *11*(4), e5432-e5432. https://doi.org/10.55251/jmbfs.5432

Fujii, T., Okuda, T., Yasui, N., Wakaizumi, M., Ikami, T., & Ikeda, K. (2013). Effects of amla extract and collagen peptide on UVB-induced photoaging in hairless mice. Journal of Functional Foods, 5(1), 451–459. https://doi.org/10.1016/j. jff.2012.11.018

Gan Z, Huang J, Chen J, Nisar MF, Qi W. Synthesis and antifungal activities of cinnamaldehyde derivatives against Penicillium digitatum causing citrus green mold. J Food Qual. 2020;2020:8898692. https://doi.org/10. 1155/2020/8898692.

Goyal, D., Saini, A., Saini, G. S. S., & Kumar, R. (2019). Green synthesis of anisotropic gold nanoparticles using cinnamon with superior antibacterial activity. *Materials Research Express*, *6*(7), 075043. DOI: 10.1088/2053-1591/ab15a6

Gupta, T., & Saxena, J. (2023). Biogenic synthesis of silver nanoparticles from Aspergillus oryzae mtcc 3107 against plant pathogenic fungi Sclerotinia sclerotiorum mtcc 8785. *Journal of microbiology, biotechnology and food sciences*, *12*(4), e9387-e9387. https://doi.org/10.55251/jmbfs.9387

Hamouda RA, Abdel-Hamid MS, Hagagy N, Nofal AM. The potent effect of selenium nanoparticles: insight into the antifungal activity and preservation of postharvest strawberries from gray mold diseases. Journal of the Science of Food and Agriculture. 2024. https://doi.org/10.1002/jsfa.13502.

Hegde, S., & Selvaraj, S. (2024). CHITOSAN: AN IN-DEPTH ANALYSIS OF ITS EXTRACTION, APPLICATIONS, CONSTRAINTS, AND FUTURE PROSPECTS. *Journal of microbiology, biotechnology and food sciences*, e10563-e10563. https://doi.org/10.55251/jmbfs.10563

Kim, H. J., Yokozawa, T., Kim, H. Y., Tohda, C., Rao, T. P., & Juneja, L. R. (2005). Influence of amla (emblica officinalis gaertn.) on hypercholesterolemia and lipid peroxidation in cholesterol-fed rats. Journal of Nutritional Science & Vitaminology, 51 (6), 413–418. https://doi.org/10.3177/Jnsv.51.413

Kumar, A., Prasad, K.S. (2021). Role of nano-selenium in health and environment. J Biotechnol. 325, 152–63. doi: 10.1016/ j.jbiotec.2020.11.004

Kunle, O. F., Egharevba, H. O., & Ahmadu, P. O. (2012). Standardization of herbal medicines-A review. *International journal of biodiversity and conservation*, *4*(3), 101-112. DOI: 10.5897/IJBC11.163

Li, Y. Q., Kong, D. X., & Wu, H. (2013). Analysis and evaluation of essential oil components of cinnamon barks using GC–MS and FTIR spectroscopy. *Industrial Crops and Products*, *41*, 269-278. https://doi.org/10.1016/j.indcrop.2012.04.056

Menon, S., Agarwal, H., Rajeshkumar, S., Rosy, P.J., Shanmugam, V.K. (2020). Investigating the antimicrobial activities of the biosynthesized selenium nanoparticles and its statistical analysis. Bionanoscience. 10, 122–35. https://doi.org/10.1007/s12668-019-00710-3

Menon, S., KS, S. D., Agarwal, H., & Shanmugam, V. K. (2019). Efficacy of biogenic selenium nanoparticles from an extract of ginger towards evaluation on anti-microbial and anti-oxidant activities. *Colloid and Interface Science Communications*, *29*, 1-8. https://doi.org/10.1016/j.colcom.2018.12.004

Najjar, K., & Abu-Khalaf, N. (2021). Visible/near-infrared (VIS/NIR) spectroscopy technique to detect gray mold disease in the early stages of tomato fruit: VIS/NIR spectroscopy for detecting gray mold in tomato. *Journal of microbiology, biotechnology and food sciences*, *11*(2), e3108-e3108. https://doi.org/10.15414/jmbfs.3108

No, H. K., Park, N. Y., Lee, S. H., & Meyers, S. P. (2002). Antibacterial activity of chitosans and chitosan oligomers with different molecular weights. *International journal of food microbiology*, *74*(1-2), 65-72. https://doi.org/10.1016/S0168-1605(01)00717-6

Noriega, P., Mafud, D. D. F., Souza, B. D., Soares-Scott, M., Rivelli, D. P., Barros, S. B. D. M., & Bacchi, E. M. (2012). Applying design of experiments (DOE) to flavonoid extraction from Passiflora alata and P. edulis. *Revista Brasileira de Farmacognosia*, *22*, 1119-1129. https://doi.org/10.1590/S0102-695X2012005000036

Oszmiański, J., & Wojdyło, A. (2009). Comparative study of phenolic content and antioxidant activity of strawberry puree, clear, and cloudy juices. *European Food Research and Technology*, *228*(4), 623-631. https://doi.org/10.1007/s00217-008-0971-2

Potrč, S., Fras Zemljič, L., Sterniša, M., Smole Možina, S., & Plohl, O. (2020). Development of biodegradable whey-based laminate functionalised by chitosan–natural extract formulations. *International journal of molecular sciences*, *21*(10), 3668. https://doi.org/10.3390/ijms21103668

Reddy, V. D., Padmavathi, P., Paramahamsa, M., & Varadacharyulu, N. C. (2010). Amelioration of alcohol-induced oxidative stress by Emblica officinalis (amla) in rats. Indian Journal of Biochemistry & Biophysics, 47, 20.

Reller, L. B., Weinstein, M., Jorgensen, J. H., & Ferraro, M. J. (2009). Antimicrobial susceptibility testing: a review of general principles and contemporary practices. *Clinical infectious diseases*, *49*(11), 1749-1755. https://doi.org/10.1086/647952

Roy, A., Bulut, O., Some, S., Mandal, A.K., Yilmaz, M.D., 2019. Green synthesis of silver nanoparticles: biomoleculenanoparticle organizations targeting antimicrobial activity. RSC Advances, 9 (5), 2673-2702.

Salem, M. F., Abd-Elraoof, W. A., Tayel, A. A., Alzuaibr, F. M., Abonama, O. M. (2022b). Antifungal application of biosynthesized selenium nanoparticles with pomegranate peels and nanochitosan as edible coatings for citrus green mold protection. *Journal of Nanobiotechnology*, *20*(1), 182. https://doi.org/10.1186/s12951-022-01393-x

Salem, M. F., Tayel, A. A., Alzuaibr, F. M., & Bakr, R. A. (2022). Innovative approach for controlling black rot of persimmon fruits by means of nanobiotechnology from nanochitosan and rosmarinic acid-mediated selenium nanoparticles. *Polymers*, *14*(10), 2116. https://doi.org/10.3390/polym14102116

Sengun, I. Y., Kirmizigul, A., & Guney, D. (2022). FRESH CUT FRUITS-AN OVERVIEW OF MICROBIOLOGICAL CONDITIONS, RECENT OUTBREAKS AND PREVENTIVE STRATEGIES. *Journal of microbiology, biotechnology and food sciences*, *12*(3), e3688-e3688. https://doi.org/10.55251/jmbfs.3688

Sharma, A., Sharma, M. K., & Kumar, M. (2009). Modulatory role of Emblica officinalis fruit extract against arsenic induced oxidative stress in Swiss albino mice. ChemicoBiological Interactions, 180(1),

Sharma, G., Sharma, A. R., Bhavesh, R., Park, J., Ganbold, B., Nam, J. S., & Lee, S. S. (2014). Biomolecule-mediated synthesis of selenium nanoparticles using dried Vitis vinifera (raisin) extract. *Molecules*, *19*(3), 2761-2770. https://doi.org/10.3390/molecules19032761

Shi, X. D., Tian, Y. Q., Wu, J. L., & Wang, S. Y. (2021). Synthesis, characterization, and biological activity of selenium nanoparticles conjugated with polysaccharides. *Critical Reviews in Food Science and Nutrition*, *61*(13), 2225-2236. doi: 10.1080/10408398.2020.1774497.

Shukla, V., Vashistha, M., & Singh, S. N. (2009). Evaluation of antioxidant profile and activity of amalaki (Emblica officinalis), spirulina and wheat grass. Indian Journal of Clinical Biochemistry, 24(1), 70–75. https://doi.org/10.1007/s12291-009-0012-3

Sonawane, S. K., Patil, S. P., & Arya, S. S. (2018). Nanotechnology enrolment in food and food safety. *The Journal of Microbiology, Biotechnology and Food Sciences*, *8*(3), 893. DOI:10.15414/jmbfs.2018-19.8.3.893-900

Tayel, A. A., Ebaid, A. M., Otian, A. M., Mahrous, H., El Rabey, H. A., & Salem, M. F. (2024). Application of edible nanocomposites from chitosan/fenugreek seed mucilage/selenium nanoparticles for protecting lemon from green mold. *International Journal of Biological Macromolecules*, 273, 133109. https://doi.org/10.1016/j.ijbiomac.2024.133109

Tayel, A. A., El-Tras, W. F., Moussa, S. H., & El-Sabbagh, S. M. (2012). Surface decontamination and quality enhancement in meat steaks using plant extracts as natural biopreservatives. *Foodborne Pathogens and Disease*, *9*(8), 755-761. https://doi.org/10.1089/fpd.2012.1203

Tayel, A. A., Elzahy, A. F., Moussa, S. H., Al-Saggaf, M. S., & Diab, A. M. (2020). Biopreservation of shrimps using composed edible coatings from chitosan nanoparticles and cloves extract. *Journal of Food Quality*, *2020*(1), 8878452.

Tayel, A. A., Ibrahim, S. I., Al-Saman, M. A., & Moussa, S. H. (2014). Production of fungal chitosan from date wastes and its application as a biopreservative for minced meat. *International Journal of Biological Macromolecules*, *69*, 471-475. https://doi.org/10.1016/j.ijbiomac.2014.05.072

Tayel, A. A., Moussa, S. H., Salem, M. F., Mazrou, K. E., & El-Tras, W. F. (2016). Control of citrus molds using bioactive coatings incorporated with fungal chitosan/plant extracts composite. *Journal of the Science of Food and Agriculture*, *96*(4), 1306-1312. https://doi.org/10.1002/jsfa.7223

Tayel, A. A., Moussa, S. H., Salem, M. F., Mazrou, K. E., & El-Tras, W. F. (2016). Control of citrus molds using bioactive coatings incorporated with fungal chitosan/plant extracts composite. *Journal of the Science of Food and Agriculture*, *96*(4), 1306-1312. https://doi.org/10.1002/jsfa.7223

Tayel, A. A., Moussa, S., Opwis, K., Knittel, D., Schollmeyer, E., & Nickisch-Hartfiel, A. (2010). Inhibition of microbial pathogens by fungal chitosan. *International journal of biological macromolecules*, *47*(1), 10-14. https://doi.org/10.1016/j.ijbiomac.2010.04.005

Tripathi, P., & Dubey, N. K. (2004). Exploitation of natural products as an alternative strategy to control postharvest fungal rotting of fruit and vegetables. *Postharvest biology and Technology*, *32*(3), 235-245. https://doi.org/10.1016/j.postharvbio.2003.11.005

Tsekhmistrenko, S. C., Bityutskyy, V., Tsekhmistrenko, O., Merzlo, S., Tymoshok, N., Melnichenko, A., ... & Yakymenko, I. (2021). BIONANOTECHNOLOGIES: SYNTHESIS OF METALS'NANOPARTICLES WITH USING PLANTS AND THEIR APPLICATIONS IN THE FOOD INDUSTRY: A REVIEW. *The Journal of Microbiology, Biotechnology and Food Sciences*, *10*(6), e1513. DOI:10.15414/jmbfs.1513

Vlčko, T., Golian, J., Fikselová, M., & Rybnikár, S. (2022). Current overview in the field of application of edible coatings/films (meat products examples). *The Journal of Microbiology, Biotechnology and Food Sciences*, *12*, e9281-e9281. https://doi.org/10.55251/jmbfs.9281

Yokozawa, T., Kim, H. Y., Kim, H. J., Okubo, T., Chu, D. C., & Juneja, L. R. (2007). Amla (Emblica officinalis Gaertn.) prevents dyslipidaemia and oxidative stress in the ageing process. British Journal of Nutrition, 97(6), 1187–1195. https://doi.org/ 10.1017/S0007114507691971

Youssef, D.M., Alshubaily, F.A., Tayel, A.A., Alghuthaymi, M.A., Al-Saman, M.A. (2022). Application of nanocomposites from bees products and nano-selenium in edible coating for catfish fillets biopreservation. *Polymers*. 14(12), 2378. https://doi.org/10.3390/polym14122378

Zhao, G., Wu, X., Chen, P., Zhang, L., Yang, C. S., & Zhang, J. (2018). Selenium nanoparticles are more efficient than sodium selenite in producing reactive oxygen species and hyper-accumulation of selenium nanoparticles in cancer cells generates potent therapeutic effects. *Free Radical Biology and Medicine*, *126*, 55-66. https://doi.org/10.1016/j.freeradbiomed.2018.07.017

Zonaro, E., Lampis, S., Turner, R. J., Qazi, S. J. S., & Vallini, G. (2015). Biogenic selenium and tellurium nanoparticles synthesized by environmental microbial isolates efficaciously inhibit bacterial planktonic cultures and biofilms. *Frontiers in microbiology*, *6*, 584. https://doi.org/10.3389/fmicb.2015.00584

Zorraquín-Peña, I., Cueva, C., Bartolomé, B., Moreno-Arribas, M., (2020). Silver nanoparticles against foodborne bacteria. Effects at intestinal level and health limitations. *Microorganisms*, 8 (1), 132. https://doi.org/10.3390/microorganisms8010132